

## HfO<sub>2</sub> based memory devices with rectifying capabilities

C. Quinteros,<sup>1</sup> R. Zazpe,<sup>2</sup> F. G. Marlasca,<sup>1</sup> F. Golmar,<sup>3,6</sup> F. Casanova,<sup>2,4</sup> P. Stoliar,<sup>5,6</sup> L. Hueso,<sup>2,4</sup> and P. Levy<sup>1</sup>

<sup>1</sup>GIA, GAIANN, CAC-CNEA, Av. Gral. Paz 1499 (1650), San Martín, Bs. As., Argentina

<sup>2</sup>CIC nanoGUNE, 20018 Donostia-San Sebastián, Basque Country, Spain

<sup>3</sup>INTI, Av. General Paz 5445 (1650), San Martín, Bs. As., Argentina

<sup>4</sup>IKERBASQUE, Basque Foundation for Science, 48011 Bilbao, Basque Country, Spain

<sup>5</sup>IMN, Université de Nantes, CNRS, 2 rue de la Houssinière, BP 32229, 44322 Nantes, France

<sup>6</sup>ECyT, UNSAM, Martín de Irigoyen 3100, B1650JKA, San Martín, Bs. As., Argentina

(Received 13 November 2013; accepted 17 December 2013; published online 8 January 2014)

We report on the fabrication and characterization of metal/insulator/metal capacitor like devices, with both rectifying and hysteretic features. Devices are formed by two junctions, Ti/HfO<sub>2</sub> and Co/HfO<sub>2</sub>. Each junction exhibits highly repetitive hysteretic I-V curves with a sharp transition from a high to a low resistance state (3–4 orders of magnitude jump). The opposite transition (from low to high) is induced by polarity reversal. The rectifying non-crossing characteristics of the I-V branches denote their potential use as a multifunctional device, acting as a built-in rectifier and memory cell in a single device. Based on the phenomenological model description by Zazpe *et al.* [Appl. Phys. Lett. **103**, 073114 (2013)], we propose a circuitual equivalent representation supported on switchable rectifying junctions. By exploring different electrode connections, we disentangle the role of the bulk transport in HfO<sub>2</sub> devices. © 2014 AIP Publishing LLC.

[<http://dx.doi.org/10.1063/1.4861167>]

Devices relying on the possibility of tuning their response with different stimulus are the focus of intense research. Magnetic, electric, optical, and tensile fields usually determine the overall response of multifunctional materials, enhancing their scope and fruitfulness. Here, we study a different kind of multifunctionality, namely the possibility to assess two different abilities on the same device, their tuning being determined by the occurrence of the driving stimulus. The sequence of applied voltage pulses, i.e., their recent history, modulates either the retention or rectifying capabilities of the device under study.

Metal/insulator/metal capacitor-like structures are prominent candidates for flash memory replacement technology, as the Resistive Switching mechanism appealing features (speed, downscaling, retention, endurance) evolve into a mature technology, coined Resistive Random Access Memory (ReRAM).<sup>1,2</sup> When transition metal oxides constitute the insulator between the metal electrodes, a huge variety of mechanisms emerge for describing memory devices with both standard and novel capabilities, evidencing the richness of this family of compounds.<sup>3,4</sup>

Rectifying metal/oxide junctions based on TiO<sub>x</sub>,<sup>5</sup> ZnO,<sup>6</sup> and on TaO<sub>2-x</sub> (Ref. 7) have been recently described, where upon appropriate oxygen vacancy accumulation the interface is switched to a non-rectifying resistive device.<sup>8</sup> The problem of sneak currents in ReRAM devices integrated in cross-bar arrays could be dealt with by the use of memory–diode devices (memdiodes).<sup>9</sup> Here, we explore rectifying HfO<sub>2</sub> based devices, having the additional built-in capability of a memory cell, both properties being tunable through electric stimulus. Specifically, in this work we propose a concentrated parameter equivalent circuit to model device's electrical response. Also, we explore an alternative electrode

configuration to check the correctness of the simple model proposed.

Samples consist of Ti(20 nm)/HfO<sub>2</sub>(20 nm)/Co(35 nm) structures fabricated using standard methods. The Ti common bottom electrode was deposited by sputtering on top of Silicon/SiO<sub>2</sub>(150 nm) substrates. Hafnium oxide films were deposited by Atomic Layer Deposition. Varying growth parameters allowed to determine the optimized conditions for obtaining highly repeatable electric response.<sup>10</sup> For the samples to be reported here, grazing incidence X-ray diffraction revealed a monoclinic phase.<sup>11</sup> Top electrodes of Co capped with Pd were further created by optical lithography and sputtering (area 200 × 200 μm<sup>2</sup> and spacing of 200 μm). In this way, in a single chip we have the common bottom electrode, hereafter referred as BE, and several top electrodes, designated as TE<sub>n</sub>, being *n* the electrode index. A Keithley 4200 source and measurement equipment connected to a standard probe station was used to electrically test devices in a shielded box at room temperature.

Figure 1 depicts a typical I-V curve obtained by sweeping voltage pulses in a two terminal electrical configuration (bias was applied to TE<sub>1</sub>, while BE was grounded). After fabrication, devices are found in High Resistance (HR) state, which abruptly switches to a Low Resistance (LR) state in a SET operation when applying a positive voltage V<sub>SET</sub> ~ 5 V. A steep 3–4 order of magnitude jump is observed. Further increasing the stimulus produces a smooth response. Upon decreasing the stimulus, the I-V curve exhibits huge hysteresis with a smooth dependence. Further cycling with positive voltages reproduces the LR state. A remarkable feature emerges as soon as polarity is reverse. Notice that, even when the positive cycle finished in a LR state, the negative voltage cycle starts in a new HR state. In other words, the

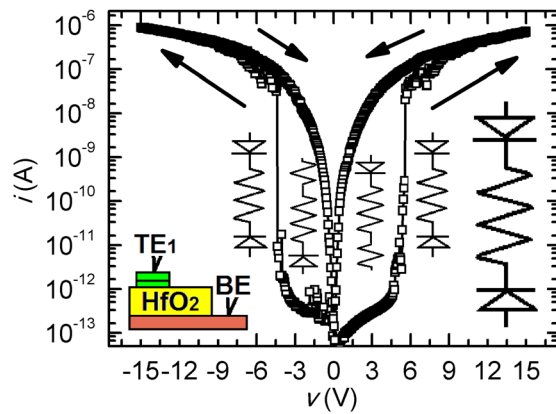


FIG. 1. I-V measurement of a Ti/HfO<sub>2</sub>/Co device using the TE<sub>1</sub> and BE electrodes at room temperature. Arrows indicate the sense of sweeping. Note the non-crossing character of the I-V curve. Insets: scheme of the measurement configuration (left) and a modelled *element* (right). Small insets near data points depict the status of the modelled *element* (see text for details).

device seems to react to a positive-negative voltage transition as if it was a rectifier changing from direct to a reverse bias regime. From that HR state on, the description of the negative voltage cycle is completely analogous to that of the positive cycle. That is to say, a SET transition occurs when a negative  $V_{\text{SET}}$  voltage is attained ( $V_{\text{SET}} \sim -5$  V) and a similar overall response is encountered when increasing/decreasing the voltage amplitude. Interestingly, when another positive cycle is started right after a negative cycle, the device presents a HR state again. Therefore, not only the rectifying effect has changed its polarization but also the device has been RESET to HR because of the negative excursion (recall the former positive cycle ended in a LR state). We say the device's hysteretic I-V response is non-crossing because the negative (positive) HR branch follows the positive (negative) LR branch.

The presence of two independently rectifying junctions, which are alternatively activated upon sweeping different polarities, gives rise to the above described non-crossing behaviour of the I-V data. When positive stimulus is applied to the TE (i.e., at the HfO<sub>2</sub>/Co junction), oxygen vacancies are accumulated near the BE (the Ti/HfO<sub>2</sub> junction) that switches from HR to LR at  $\sim 5$  V. Upon polarity reversal, the rectifying character of the TE comes into play; at  $\sim -5$  V, the oxygen vacancies driven to the HfO<sub>2</sub>/Co junction produce the switching from HR to LR. Recently, a model based on switchable HfO<sub>2</sub>/metal interfaces was used to thoroughly describe electrical response of similar samples.<sup>10</sup>

Interestingly, the response of the LR state at the highest fields studied here for both polarities (namely  $\pm 15$  V) is a relatively high resistance ( $\sim 3 \times 10^7 \Omega$ ), and does not show any signature of dielectric breakdown though the acting electric field surpasses  $10^9$  V/m. Besides, the LR state exhibits a highly non-ohmic character: by fitting I-V data with the expression  $V \sim I^\alpha$  gives  $\alpha \sim 1/2.7$  for both positive and negative polarities.

We explored both HR and LR states by checking remnant states with a reading bias voltage of +3 V. Figure 2 exhibits the response of the sample to a pulsed write/erase protocol. Voltage stimulus corresponding to a SET/read/RESET/read

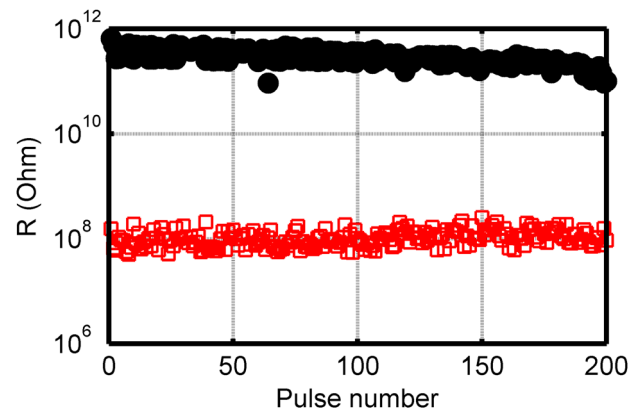


FIG. 2. Reading at +3 V after write/erase pulsed operations, exhibiting the switching capability of the Ti/HfO<sub>2</sub>/Co device. The following sequence of pulses (100 ms of duration) of different amplitudes was applied at room temperature: SET (+10 V)/read (+3 V)/RESET (-3.5 V)/read (+3 V).

sequence was applied around 200 times, with an ON/OFF ratio of 3–4 orders of magnitude, and negligible degradation. These findings promote the multifunctional capabilities of Ti/HfO<sub>2</sub>/Co structures as rectifying and retentive devices. The above described behaviour can be qualitatively modelled, with a circuitual equivalent representation, assuming that each metal/oxide interface behaves like a hysteretic rectifying junction, which can be turned into a (non-ohmic) resistive device upon appropriate SET/RESET operations. Besides, the bulk contribution of the HfO<sub>2</sub> layer is also to be considered. Therefore, this *transverse* configuration (contacting TE<sub>1</sub> and BE) is modelled as two (switchable) diodes in an opposite polarity configuration (i.e., back to back series connection) with a series resistance in between them, as depicted in Fig. 1 (right inset). The diodes represent both injection barriers, while the resistance stands for the bulk HfO<sub>2</sub> contribution.

Hereafter, this model device will be referred to as an *element*. For small positive voltage, one diode is forward biased, while the other one, which is reverse biased, prevents the current flow giving rise to the HR state. At  $V_{\text{SET}}$ , the reverse biased diode becomes a conducting non-ohmic resistance and the LR state of the *element* is mainly limited by the bulk resistance. Upon decreasing the applied voltage, the LR state remains active, as the diode switched irreversibly into a non-ohmic resistance (see the small insets in Fig. 1).

For negative voltage, the role of both diodes is interchanged, with a similar qualitative overall response: as soon as polarity is inversed, the formerly switched diode at BE switches back (as vacancies are expelled), and the diode at TE remains reverse biased until the negative  $V_{\text{SET}}$  is reached, switching it to a non-ohmic resistance.

In order to experimentally check the correctness of such concentrated parameter equivalent circuit, we tested a measurement configuration consisting of two such *elements* in a serial connection. The *series*<sup>12</sup> configuration can be performed on a single sample, as the metallic BE is common to all devices, and connects *transverse* devices as depicted in Fig. 3 (right inset). Top electrodes acting as Bias and Ground are labelled TE<sub>1</sub> and TE<sub>2</sub> contacts, respectively.

Fig. 3 shows a comparison of measurements performed in the *transverse* and in the *series* configurations. The

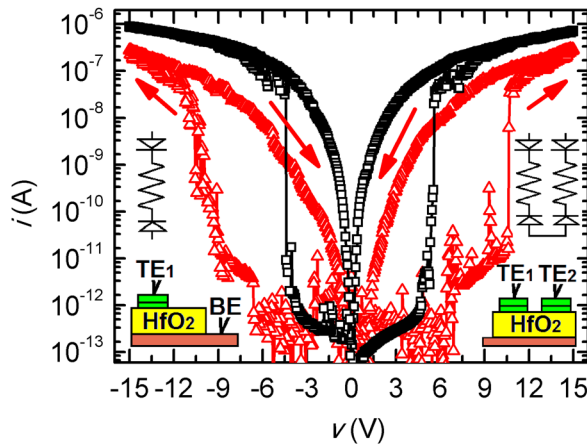


FIG. 3. Comparison of I-V measurements performed in the *transverse* (open squares) and in the *series* (open triangles) configuration for the Ti/HfO<sub>2</sub>/Co sample at room temperature. Arrows indicate the sense of sweeping. A non-crossing behaviour is observed in both cases. Left inset: scheme of the *transverse* configuration and the modelled *element*. Right inset: scheme of the *series* measurement configuration and two model *elements* in series.

general trend of both measurements displays steep SET transitions and a smooth saturation behaviour for the LR states. Quantitative changes are observed: the  $V_{\text{SET}}^{\{\text{series}\}}$  and the  $V_{\text{SET}}^{\{\text{transverse}\}}$  values are +10 V and +5 V for positive polarity, and -8 V and -5 V for negative polarity, respectively. Besides, the saturation resistance value (say, resistance at 15 V) is higher in the *series* connection than in the *transverse* one. These extra contributions are clearly related to the presence of two *elements* in a back to back series connection, which renders the overall device harder to switch.

A shorting path through the bulk HfO<sub>2</sub> may also link these *elements*. To test for such possibility, we performed *series* measurements of distant top electrodes in order to deliberately increase this suspected linking bulk resistance contribution. Several TE<sub>1</sub>-TE<sub>n</sub> measurement configurations were studied, where “n” is a label that stands for numbering neighbouring devices, each one separated from the following one by a spacing of  $\Delta x = x(\text{TE}_{n+1}) - x(\text{TE}_n) = 200 \mu\text{m}$ , and adding a link contribution  $R_L$ .

Figure 4 depicts the resistance data for different *series* measurements, as extracted from the current measured at +15 V. The resistance of these different configurations is reported as a function of the distance between the top electrodes TE<sub>0</sub> - TE<sub>n</sub>.

At  $n=0$ , the depicted measurement is the *transverse* configuration (i.e., data obtained using contacts at TE<sub>0</sub> and BE). It is reported for comparison, giving the appropriate quantitative scale range. For  $n > 1$ , as the distance between electrodes increases,  $R(n)$  increases smoothly, reaching the saturation level for  $n > 4$ . The dependence shown in Fig. 4 supports a scenario where *elements* are connected not only through the common BE but also through a bulk linking path that becomes significant for small  $n$ . Although as the series connection increases top electrodes’ distance, remaining current flow through this path is reduced.

Note that we can safely rule out the possibility of a surface contamination, which could establish a non-bulky path:

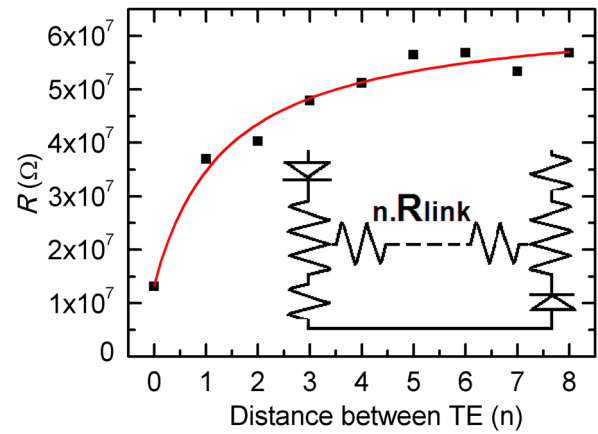


FIG. 4. Comparison of the resistance at +15 V ( $V/I$  at +15 V) for different *series* measurements using the TE<sub>0</sub>-TE<sub>n</sub> configurations for the top electrodes. The measurement TE<sub>0</sub> stands for the *transverse* measurement using contacts at TE<sub>0</sub> and BE. The inset depicts a scheme of the concentrated parameter model for the *series* configuration.

the switch at the BE in the I-V data of the *series* configuration is indeed observed at a value  $V_{\text{SET}}^{\{\text{series}\}}$ , which is greater than the  $V_{\text{SET}}^{\{\text{transverse}\}}$  one. This fact confirms that a fraction of the injected current traverses perpendicularly two *elements* and does not short circuit both TEs through the surface of the device.

We performed a fitting of the data assuming a concentrated parameter equivalent circuit<sup>13</sup> in which a fixed  $R_L$  value is added “n” times when measuring at position “n” (see Fig. 4 inset). The fitting expression was obtained by solving the equivalent circuit as a function of “n.” The obtained expression is  $R(n) = P1 \cdot n / (P2 \cdot n + 1) + P3$ , where  $P1$ ,  $P2$ , and  $P3$  are parameters relating  $R_L$  to the other non-ohmic resistance values.<sup>13</sup> From the fitting procedure (which does not include the data at  $n=0$ , as it was measured in the *transverse* configuration), we obtain  $R_L \sim 40 \text{ M}\Omega$ . Note that this value is a parameter extracted from the LR response measured at 15 V, as the LR state I-V data exhibit a highly non linear behaviour. The obtained  $R_L$  value is  $\sim 3$  times higher than the *transverse* resistance (measured at 15 V). This fact allows understanding the initial dependence with the TE distance in the  $n < 3$  range. As the distance between electrodes increases, the resistance grows smoothly reaching a saturation level for larger values ( $n > 4$ ). These results validate the rather simple modelling of Ti/HfO<sub>2</sub> and HfO<sub>2</sub>/Co interfaces as diodes connected through a bulk resistance contribution, mainly arising from HfO<sub>2</sub>. The *series* connection measurement provided qualitative and quantitative support for this modelling scheme.

The presence of two rectifying junctions connected back to back suggests new functionalities. In our case, memory features added to rectifying capabilities in both polarities may open the possibility to tackle snake-path problems in crossbar integrated devices without going beyond the  $4F^2$  cell design of standard MIM structures.<sup>4,6</sup> Besides, these HfO<sub>2</sub> based devices exhibit low ( $\sim 0.5 \mu\text{W}$ ) power consumption for each write/read operation, i.e., lower than standard memory cells based on the resistive switching of bulk

HfO<sub>2</sub>.<sup>14</sup> In our case, the combination of rectifying and retentive features emerges due to the presence of two main factors. First, the occurrence of a high electric field at the metal-oxide junctions that drives back and forth the vacancies<sup>10</sup> and determines the memristive features of the device, with an ON/OFF ratio of 3–4 orders of magnitude. Central to this aspect is the high resistivity of the “bulk” HfO<sub>2</sub> material. The concentrated parameter equivalent circuit presented and discussed above allowed to disentangle interface from bulk contributions to the total resistivity of the device. Second, the unique rectifying capabilities demonstrated by the Ti/HfO<sub>2</sub> and Co/HfO<sub>2</sub> junctions, which can be modelled as rectifying switchable junctions.<sup>10</sup>

In conclusion, we fabricated and characterized the electrical response of Ti/HfO<sub>2</sub>/Co multifunctional rectifying memory devices. They exhibit highly repetitive hysteretic I-V curves, with sharp SET and smooth RESET transitions, with non crossing type response. A simple model based on switchable diodes and resistances was used to account for this behaviour, obtaining evidence for non-crossing remnant I-V response and non-trivial HfO<sub>2</sub> bulk electronic transport. The rectifying character with remnant features of these devices may allow integrating them in a combined way as multifunctional devices. The use of HfO<sub>2</sub> as the insulator envisages their integration with CMOS standard silicon based planar technology.

Support from CONICET (PIP-047 “MEMO”) and MeMOSat Project (DuPont-CONICET and INNOVAR2012) is acknowledged. F.G. and P.L. are members of CONICET. C.Q., a Ph.D. student of the University of Buenos Aires, gratefully acknowledges economical support of a CONICET grant.

<sup>1</sup>R. Waser and M. Aono, *Nature Mater.* **6**, 833 (2007).

<sup>2</sup>M. Rozenberg, *Scholarpedia* **6**(4), 11414 (2011).

<sup>3</sup>R. Waser, R. Dittmann, G. Staikov, and K. Szot, *Adv. Mater.* **21**, 2632 (2009).

<sup>4</sup>J. Joshua Yang *et al.*, *MRS Bull.* **37**, 131 (2012); J. Joshua Yang, D. B. Strukov, and D. R. Stewart, *Nat. Nanotechnol.* **8**, 13 (2013).

<sup>5</sup>N. Zhong, H. Shima, and H. Akinaga, *Appl. Phys. Lett.* **96**, 42107 (2010).

<sup>6</sup>A. Shih, W. Zhou, J. Qiu, H. J. Yang, S. Chen, Z. Mi, and I. Shih, *Nanotechnology* **21**, 125201 (2010).

<sup>7</sup>M.-J. Lee, C. B. Lee, D. Lee, S. R. Lee, M. Chang, J. H. Hur, Y.-B. Kim, C.-J. Kim, D. H. Seo, S. Seo, U.-I. Chung, I.-K. Yoo, and K. Kim, *Nature Mater.* **10**, 625–630 (2011).

<sup>8</sup>S. D. Ha and S. Ramanathan, *J. Appl. Phys.* **110**, 071101 (2011).

<sup>9</sup>S. Saraf, M. Markovich, T. Vincent, R. Rechter, and A. Rothschild, *Appl. Phys. Lett.* **102**, 022902 (2013).

<sup>10</sup>R. Zazpe, P. Stoliar, F. Golmar, R. Llopis, F. Casanova, and L. E. Hueso, *Appl. Phys. Lett.* **103**, 073114 (2013).

<sup>11</sup>K. Kukli, T. Pilvi, M. Ritala, T. Sajavaara, J. Luc, and M. Leskelä, *Thin Solid Films* **491**, 328 (2005).

<sup>12</sup>K. M. Kim, B. J. Choi, Y. C. Shin, S. Choi, and C. S. Hwang, *Appl. Phys. Lett.* **91**, 012907 (2007).

<sup>13</sup>See supplementary material at <http://dx.doi.org/10.1063/1.4861167> for details on Fig. 4's fitting expression.

<sup>14</sup>H.-Y. Lee, P.-S. Chen, C.-C. Wang, S. Maikap, P.-J. Tzeng, C.-H. Lin, L.-S. Lee, and M.-J. Tsai, *Jpn. J. Appl. Phys., Part 1* **46**, 2175 (2007).